Journal of Hydrology 517 (2014) 949–962

Contents lists available at ScienceDirect

Journal of Hydrology

journal homepage: www.elsevier.com/locate/jhydrol

# Linkages between snow ablation and atmospheric boundary-layer conditions in a semi-arid basin of Western Canada

Scott I. Jackson *, Terry D. Prowse, Barrie R. Bonsal

*Water and Climate Impacts Research Centre (W-CIRC), Environment Canada, Department of Geography, University of Victoria, Victoria, British Columbia V8W 3R4, Canada*

ARTICLE INFO

*Article history:*
Received 13 December 2013
Received in revised form 28 May 2014
Accepted 7 June 2014
Available online 18 June 2014
This manuscript was handled by Konstantine P. Georgakakos, Editor-in-Chief, with the assistance of Kun Yang, Associate Editor

*Keywords:*
Snow melt
Atmospheric boundary layer
Radiosonde
Trends
Teleconnections
Okanagan

SUMMARY

High-elevation snowpacks provide critical inputs to the hydrological system of mountainous semi-arid regions where summer precipitation is insufficient to maintain adequate discharges for ecological and economic needs. The Okanagan Basin in Western Canada is an example of such a system, as most of the summer streamflow is derived from snowmelt. To better understand how snowmelt events vary as a result of atmospheric conditions, this study developed statistical models using upper-air atmospheric data for evaluating changes in snowpack ablation. Specifically, radiosonde data were statistically linked with detailed ground-based measurements of snowmelt and associated streamflow. Statistical models were developed based on data from the 2007 ablation season and concurrent data from the 850 hPa geopotential height. These models explained 57–68% of the variance in snowmelt for 2007, and were extended to predict snowmelt for the radiosonde period of record (1972–2012). Time-series analyses showed significant trends toward higher winter and spring temperatures, vertical temperature gradients in the atmospheric boundary layer in spring, and earlier dates for snowmelt and freshet initiation. Significant negative trends were also found towards decreasing spring precipitation. More broadly, ablation-season climatic and hydrological variables were significantly positively correlated with the winter and spring Multivariate El Niño Southern Oscillation and Pacific Decadal Oscillation indices, in which the positive (negative) phase was associated with higher (lower) magnitude and frequency of melt events. This combination of strong correlations and significant temporal trends indicates that with projected air-temperature increases, the magnitude and duration of melt events are likely to increase, particularly during favourable phases of the above teleconnections.



## 1. Introduction

Water resources in semi-arid regions with high-elevation snowpacks, are highly susceptible to changes in snowmelt timing and volume as this process maintains stream flows throughout the dry summer months (Barnett et al., 2005). Given the strong reliance of these regions on vulnerable high-elevation snowpacks, it is critical that snow ablation processes and their links to the controlling meteorological conditions are better understood. This is particularly true for the Okanagan Basin in south-central British Columbia, where the stress on fresh-water supplies is increasing due to increasing population and a changing climate (Fig. 1). The Okanagan Basin is already undergoing substantial hydro-climatic change. Over the past century, in the Coldstream sub-basin both winter and spring temperatures and winter, spring, autumn and annual precipitation have increased significantly (Taylor and Barton, 2004). This coincides with a shift towards a two days/decade (1901–2012) earlier occurrence of the spring 0 °C isotherm at the Vernon Coldstream Ranch station in the northern portion of the Okanagan Basin (Bonsal and Prowse, 2003). Future climate projections indicate that over the next century as winter temperature and precipitation increase, less precipitation will fall as snow and the snowmelt season will occur 4–6 weeks earlier, resulting in "considerable reductions" in annual and spring flow volumes (Merritt et al., 2006).

Further compounding stress on the hydrologic regime are the extensive forest cover changes resulting from a mountain pine-beetle epidemic. In particular, snow accumulation and ablation patterns are projected to change as openings in the forest become larger and more interconnected, thereby increasing snow accumulation, fetch lengths and melt rates (Carroll et al., 2006; Boon, 2009).

Information about snow energy and mass exchanges at higher elevations in the Okanagan is limited, making evaluation of

* Corresponding author. Present address: BC Ministry of Environment, Bag 5000, 3726 Alfred Avenue, Smithers, BC V0J 2N0, Canada. Tel.: +1 250 847 7507; fax: +1 250 847 7591.
*E-mail address:* Scott.Jackson@gov.bc.ca (S.I. Jackson).

http://dx.doi.org/10.1016/j.jhydrol.2014.06.010
0022-1694/

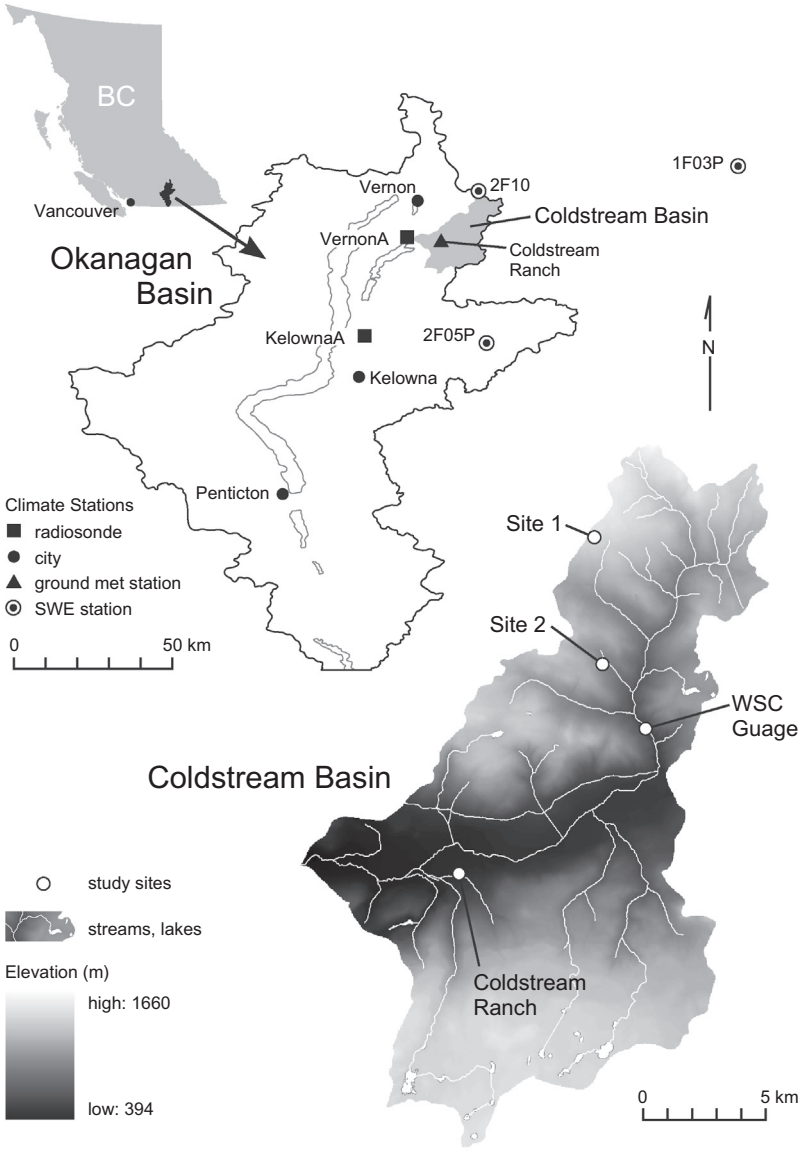


**Fig. 1.** Location of Coldstream Basin within British Columbia, Canada, and climate stations used in the analysis.

atmospheric-change effects challenging (Merritt et al., 2006). The lack of information partly stems from the high cost of long-term maintenance of high-elevation climate stations. As an alternative, this study explored the use of upper atmosphere climate data obtained from operational radiosonde flights, to evaluate long-term changes in the ablation-season snow energy balance. This required detailed ground-level information on snow melt processes from which statistical relationships with atmospheric data could be established. Such information was available from a previously published study (Jackson and Prowse, 2009) in which snow ablation processes were investigated along a four-site elevational transect in a high-elevation basin situated at the north end of the larger Okanagan Basin.

The issue of scale is paramount in snow hydrology, and in particular, the scaling up of site-specific data to accurately represent basin-wide responses (Blöschl, 1999). Given the operational impracticality of conducting snow ablation measurements at multiple sites for many years, it is necessary to find alternative methods to estimate snow melt over larger spatial and temporal scales. Radiosonde flights take measurements throughout the atmospheric boundary layer (ABL) profile, which mitigates some of the influence of site-specific factors such as vegetation and topography. Above a certain elevation (dependant on the depth of the boundary layer), the influence of spatial variation in topography and vegetation at the micro- and meso-scale becomes muted, and the conditions measured in the ABL integrate the effects of the composition of the earths surface on the atmosphere over a much wider area. Therefore, the radiosonde data provide an excellent source of high-quality data that can be considered representative of the northern Okanagan Basin.

Although the literature regarding use of radiosonde data to characterise surface energy balance is limited, there are several studies that have examined the utility of this approach. For example, Granger and Male (1978) reported that sensible heat flux over a melting snowpack in Saskatchewan was more closely related to the 850 hPa height temperature than near-surface temperature. This was due to advection from the air mass dominating the ground level sensible heat flux instead of local radiative heating and advection (e.g., from snow free areas). Additional studies have shown that evaporation estimates derived from radiosonde data provided good agreement with ground based measurements over a wide area, in both simple (Mawdsley and Brutsaert, 1977;

Sugita and Brutsaert, 1991, 1992) and complex terrain (Kustas and Brutsaert, 1986; Brutsaert and Kustas, 1987). Finally, several studies have defined linkages between conditions in the atmospheric boundary layer and regional scale variations in streamflow (e.g., Cayan and Peterson, 1989; Kim et al., 2010).

Upper atmosphere data allow the characterisation of the hydrological cycle over much broader spatial and temporal scales than point scale climate station data do, and have great potential for use in estimating streamflow generation mechanisms in ungauged basins. Based on these findings, this study seeks to determine whether statistical models based on radiosonde data are capable of predicting measured snowmelt and melt driven streamflow at the basin scale; whether these results can be used to extend the period of record of melt events; and then to determine the existence and magnitude of trends in the extended record, and linkages to teleconnection indices.

Ongoing and projected climatic changes have resulted in substantial alterations to the hydrological cycle and this appears to be intensifying (Huntington, 2006; Lemke et al., 2007; Durack et al., 2012). Evidence of a changing climate is often first noticed in high-elevation and high-latitude areas, where even slight increases in air temperature can have large impacts on hydrologic systems. In particular, increasing frequency and magnitude of flood and drought events, decreasing water storage in Northern Hemisphere snowpacks, and a shift towards earlier and more intense snowmelt have already been observed and are projected to continue, with more pronounced shifts at higher elevations and latitudes (e.g., Adam et al., 2009). One direct result of earlier snowmelt initiation is a shift towards earlier dates of maximum spring runoff and reduced summer streamflows (Déry et al., 2009). In Canada, annual mean streamflow has decreased significantly in the southern regions since 1947, with the strongest declines in August and September, whereas March and April discharge has exhibited significant increases, particularly in British Columbia (Zhang et al., 2001). Two separate studies reported that shifts towards earlier peak flows and a spring pulse onset of 10–30 days are common in basins less than 2500 m in elevation (Regonda et al., 2005; Stewart et al., 2005). A more recent study found that while snowmelt dominated regimes continue shift earlier in the year, a clear signal of accelerating change in the last decade was not evident (Fritze et al., 2011).

Due to the importance of seasonal snowpacks in the functioning of many terrestrial and climatic systems, much effort has been directed towards discerning the linkages between climate anomalies and snowpack variability (e.g., Clark et al., 2001; Stahl et al., 2006; Bao et al., 2011), and the ongoing and predicted effects of anthropogenic climate change (e.g., Räisänen, 2008; Vavrus, 2007; Bavay et al., 2009). A consistent conclusion regarding 20th century North American snow cover and ablation is that variability has increased, ablation is occurring earlier and in some cases more rapidly, with a concurrent shift towards decreased snow-cover duration at lower elevations (Déry and Brown, 2007; Dyer and Mote, 2007; Brown and Mote, 2009; McCabe and Wolock, 2010). These changes have been directly linked to an increase in spring air temperatures, with some variability at smaller spatial scales due to inter-decadal variation in precipitation, as well as elevation and latitude effects on temperature and therefore precipitation phase (Mote, 2003; Hamlet et al., 2005). In addition to the influence of changing air temperatures on snow in western North America, a significant proportion of inter-annual to inter-decadal variability in snow cover, melt and water equivalence is explained by the oscillations of several Pacific-related teleconnection indices including El Niño – Southern Oscillation (ENSO) and the Pacific Decadal Oscillation (*PDO*) (e.g., Brown and Goodison, 1996; Moore and McKendry, 1996; Hsieh and Tang, 2001; McCabe and Dettinger, 2002; Jin et al., 2006; Romolo et al., 2006a,b).

These findings highlight an ongoing research need for the detection and understanding of hydro-climatic trends and variability at high elevations and in small basins (<100 km$^2$) (McCabe and Clark, 2005; Déry and Brown, 2007; de Jong et al., 2009; Stewart, 2009).

Given the issues outlined above, the objectives of this study are to:

(1) assess the degree to which measurements collected by radiosonde are representative of meteorological conditions at the snow surface during the 2007 ablation season;
(2) develop statistical relationships between upper-air atmospheric and ablation-season snow-surface energy exchanges in a sub-basin of the Okanagan Basin;
(3) employ the resulting statistical models to evaluate snowmelt events over the longer term atmospheric data record; analyse time-series of measured and indexed hydrometeorological variables associated with such events, and;
(4) assess their relationships with large-scale teleconnection patterns.

The representative 2007 ablation season included a range of melt events, of varying magnitude, controlled by a broad range of meteorological conditions (Jackson and Prowse, 2009). This comprehensive field data set offers a unique chance to study the linkages between surface and atmospheric boundary layer (ABL) processes, and to extend the record of snow melt events using the available radiosonde record.

The analysis is presented as follows: Section 2 describes the study area and data sources; Section 3 outlines the evaluation of the data sets used, the snow melt models constructed from these data and their verification, and the methods used to assess trends and linkages to the dominant teleconnection indices, and; Section 4 presents the results of the trend and teleconnection analyses.

## 2. Study area and data

### 2.1. Study area

Covering an area of 8046 km$^2$, the Okanagan Basin comprises a portion of the northern Columbia River Basin (Fig. 1). The region is characterised by a dry continental climate, with precipitation averaging 250–300 mm in the valley and >1000 mm at higher elevations, with an estimated 85% of the total lost to evapotranspiration at lower elevations. Average annual air temperature decreases, and precipitation and snowpack increase along a south to north transect within the basin, with the southern section containing Canada's only true desert ecosystem (Cohen and Kulkarni, 2001). The valley bottoms are classified as semi-arid, and subject to increasing water stress as irrigation, agriculture and municipal growth expand (Cohen and Neale, 2006).

This study focused on the Coldstream basin, which is located at the northern end of the Okanagan Basin, because of the unique availability of the detailed snow energy balance data and the density of high-quality, long term climatic and hydrometric records (Table 1 and Fig. 1; Jackson and Prowse, 2009). The Coldstream basin ranges in elevation from 480 to 1460 masl, covering 58.5 km$^2$. The Vernon Coldstream Ranch station climate normals show a mean air temperature of the coldest month at −5.0 °C, the warmest month 19.1 °C, and the average annual precipitation of 484.4 mm, with 127.9 mm of that falling as snow (Environment Canada, 2012b). Maximum annual snow water equivalent (SWE) in the northern portion of the basin averages 733 mm and 998 mm by early May for the Silver Star snow course (2F10; BC River Forecast Centre; http://bcrfc.env.gov.bc.ca/data/) and Park Mountain snow pillow (1F03P) respectively (Table 1;

**Table 1**
Data sources for Coldstream Basin, British Columbia. $T_{wet}$ = wet bulb temperature, $T_{dry}$ = dry bulb temperature, $P$ = atmospheric pressure, $U_{dir}$ = wind direction, $SD$ = snow depth, $PC$ = precipitation.

| Station | Site ID | Type | Record period | Elevation (masl) | Variables |
|---|---|---|---|---|---|
| Vernon | 1128582 | Climate-AHCCD | 1900–2011 | 427 | $T_a$ (*max, min, mean*) |
| Vernon Bella Vista | 1128553 | Climate-AHCCD | 1900–2010 | 427 | *PC* |
| Coldstream Creek | 08NM142 | Hydrometric | 1967–2011 | 620 | *Q* |
| Coldstream Ranch | 1128581 | Climate | 1991–2012 | 482 | $T_{wet}$, $T_{dry}$, *RH*, *U*, $U_{dir}$, *P* |
| Kelowna A | 1123970 | Climate | 1971–2008 | 430 | $T_{wet}$, $T_{dry}$, *RH*, *U*, $U_{dir}$, *P* |
| Vernon | 1128551 | Climate | 1971–1995 | 556 | $T_{wet}$, $T_{dry}$, *RH*, *U*, $U_{dir}$, *P* |
| Coldstream Up | Site 1 | Climate | 2007 | 1456 | $T_a$, *RH*, *U*, $U_{dir}$, $R_N$, $\Delta T_S$, *SD*, *SWE* |
| Coldstream Mid | Site 2 | Climate | 2007 | 980 | $T_a$, *RH*, *U*, $U_{dir}$, $R_N$, $\Delta T_S$, *SD*, *SWE* |
| Kelowna Airport | 71203 | Radiosonde | 1994–2012 | 456 | $T_a$, *RH*, *e*, *Z*, *U*, $U_{dir}$, *P* |
| Vernon Airport | 71115 | Radiosonde | 1972–1993 | 556 | $T_a$, *RH*, *e*, *Z*, *U*, $U_{dir}$, *P* |
| Silver Star Mtn. | 2F10 | Snow Course | 1959–2012 | 1840 | *SWE*, *SD* |
| Park Mtn. | 1F03P | Snow Pillow | 1985–2011 | 1857 | *SWE* |
| Mission Creek | 2F05P | Snow Pillow | 1970–2011 | 1794 | *SWE* |

Fig. 1). In 2007, the March–April mean temperature at Coldstream Ranch was 6.9 °C compared to the 1970–2000 normal of 5.7 °C, and the April 1 SWE value at Silver Star Resort was 98% of the historical average.

### 2.2. Snow energy balance and upper air data

Snow melt [$Q_M$] was quantified for the 2007 ablation season based on the results from two study locations examined in Jackson and Prowse (2009): Site 1 (1450 m) and Site 2 (980 m) (Fig. 1 and Table 1). These data were collected at the field sites from February 13 – April 19, 2007 and included the following parameters: wind speed and direction, air temperature, relative humidity, net radiation, incoming and outgoing longwave and shortwave radiation and snow temperature and density profiles. Melt rates were estimated with the SNTHERM model (Jordan, 1991) driven by micro-meteorological data at both sites, and verified using concurrent daily gravimetric (lysimeter) and snow course measurements. At Site 1, the SNTHERM melt estimates [$Q_{M1}$] compared well with the gravimetric measurements ($R^2 = 0.71$), but the relationship was poorer for Site 2 ($R^2 = 0.25$). This result was attributed to either incomplete drainage of melt water from the lysimeters or advection from nearby vegetation which is not parameterized in the SNTHERM model (Jackson and Prowse, 2009). Radiosonde data were downloaded from the Integrated Global Radiosonde Archive (IGRA; Durre et al., 2006; Durre and Yin, 2008) for the closest stations in the Okanagan Basin: the Vernon Airport for 1972–1994 and, due to station relocation, the Kelowna Airport for 1994–2012 (Table 1 and Fig. 1).

## 3. Methods

### 3.1. Evaluation of data representativeness

Snowmelt and surface energy balance data collected during the 2007 ablation season were statistically linked to radiosonde data for the same period. These statistical models were used to extend the record of snowmelt events in the Coldstream Basin for the period 1972–2012. To ensure that the radiosonde data were representative of atmospheric conditions prevailing over the Coldstream study site during the 2007 ablation season, the relevant parameters recorded at Sites 1 and 2 (air temperature [$T_a$], relative humidity [*RH*], wind speed [*U*], vapour pressure [*e*] and saturated vapour pressure [$e_s$]) were correlated with the 850 hPa height data (Table 2 and Fig. 2). These measurements represented the atmospheric conditions for a 12 h period centred on the radiosonde measurement intervals (00 and 12 UTC), and all snow surface meteorological variables were averaged over the same interval.

**Table 2**
Correlations between meteorological variables measured at Sites 1 and 2 during the ablation season of 2007, and the same variables at the 850 hPa height in the radiosonde record. Comparison conducted at a 12 h time step.

| Site 1 | | Site 2 | |
|---|---|---|---|
| Variable | *r* | Variable | *r* |
| $T_a$ | 0.97 | $T_a$ | 0.92 |
| *RH* | 0.85 | *RH* | 0.79 |
| $e_s$ | 0.97 | $e_s$ | 0.92 |
| *e* | 0.94 | *e* | 0.91 |
| *U* | 0.36 | *U* | −0.04 |

$T_a$, *RH*, *e* and $e_s$ from the 850 hPa height were significantly correlated with the same variables measured above the snow surface at Sites 1 and 2; indicating that radiosonde data are robust surrogates for surface level measurements (Table 2 and Granger and Male, 1978). $T_a$ and $e_s$ at 850 hPa averaged 5.4 °C and 9.2 hPa during high magnitude melt events (>10 mm $d^{-1}$; Fig. 3). The $e_s$ gradient lessens between the 700 and 500 hPa geopotential heights (0.01 $e_s$ hPa/geopotential hPa), compared to the gradient between the 850 and 700 hPa geopotential heights (0.04 $e_s$ hPa/geopotential hPa).

For this type of analysis, the choice of which pressure level to use has an impact on the representativeness of the models developed from the radiosonde data. This study assessed the 850 hPa and 700 hPa heights and decided to incorporate the former since correlations between ground level and radiosonde measurements were higher for the 850 hPa height for all variables (26% higher for Site 1, and 52% higher for Site 2) except zonal and meridional wind speed, which had only marginally higher correlations at the 700 hPa height. The 850 hPa readings are taken at an elevation close to the local height of land, and are therefore likely to be influenced by (and more representative of) the surrounding topography, while the 700 hPa readings are approximately 1500 m higher, and more representative of the synoptic wind conditions.

Wind speed is an important control on the turbulent transfer of sensible and latent heat at the snow surface, but correlations between surface and ABL data were poor, likely due to topographical modification of the wind field (Table 2 and Fig. 2; Jackson and Prowse, 2009). Wind direction has a bimodal distribution at Site 1 (SSW and NE), and a unimodal distribution at the other two field sites and at the 700 and 850 hPa heights (Fig. 4). Wind direction (SW) is similar for Site 2 and the two radiosonde levels, but markedly different for the Coldstream Ranch site. The latter site is subject to prevailing outflow winds from the mountainous terrain to the east. Site 2 was located on the western slope of the Coldstream drainage in the lee of the eastern slopes of the basin, and is therefore sheltered from the outflow winds (Fig. 1). Site 1 is situated

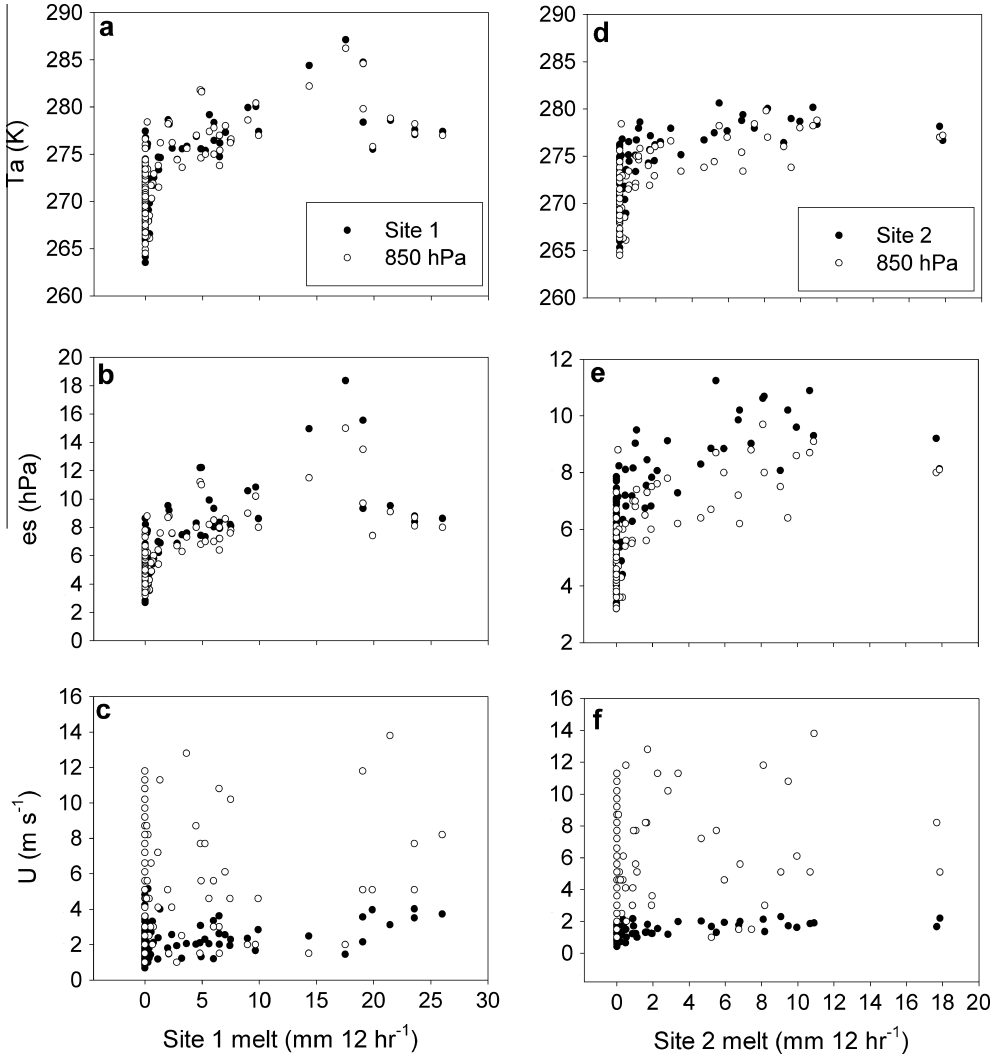


**Fig. 2.** 12 h melt totals for Site 1 and; (a) $T_{a850}$, (b) $e_{s850}$, (c) $U_{850}$, and 12 h melt totals for Site 2 and; (d) $T_{a850}$, (e) $e_{s850}$ and, (f) $U_{850}$. Melt rate is plotted on the *x*-axis.

higher in the basin, and the bimodal wind direction is likely due to the competing influences of the easterly outflows, and the synoptic south-westerly flows as evident in the radiosonde data. Meridional and zonal winds are retained as significant predictors in the melt models for Site 1, but not for Site 2 (Section 3.2). The weighting assigned to the wind variables are much lower relative to temperature and saturated vapour pressure at Site 1.

Consideration of bias in the radiosonde data when compared to the surface climate data is also important. In this case, bias in the climatic parameters was not unidirectional, and sufficient surface level data does not exist to derive a robust bias correction algorithm. The overall objective was to derive relationships between the surface and atmospheric conditions that were representative of the basin scale hydrological response. Therefore, the key metrics for evaluation of the models performance are the ability to replicate the regional snowmelt and streamflow measurements (timing and magnitude, not absolute values), and on the identification of trends, and correlations with teleconnections.

The radiosonde release point was changed in 1994 from the Vernon Airport to the Kelowna Airport. To determine whether this resulted in a significant step change three analyses were conducted. First, daily average values of $T_a$ and *RH* from the 850 hPa height were correlated with the same parameters measured at the Coldstream Ranch climate station for the period 1972–2012 to determine if the 1994 relocation of the radiosonde station significantly changed the relationship between the upper-air and ground-level climate variables (Gaffen et al., 2000). Missing data (eight days) were estimated using lapse rates between the Coldstream Ranch station and the radiosonde data. Second, the distribution and variance of the predictor variables ($T_{a850}$, $\Delta T_{a850}$, $e_{s850}$, $MW_{850}$, $ZW_{850}$) were tested for significant differences in distribution between the release sites, using the Kolmogorov–Smirnov test. The cumulative frequency distributions for the predictor variables are presented in Fig. 5. Third, a Pettitt change point test (Pettitt, 1979) was run for each variable to determine whether there was a detectable change point, and if so, whether it corresponded to the station move. The Pettitt test was chosen as it is more sensitive to breaks in the middle of the time-series, is non-parametric, and is less sensitive to outliers than other similar change point tests (Wijngaard et al., 2003).

The effect of the radiosonde station move in 1994 had no discernible effect on the distribution of $T_{a850}$ or $e_{s850}$, as neither parameter had statistically significant differences in distribution between the two release points (Fig. 5), and daily average temperature and relative humidity from the radiosonde record and the Coldstream Ranch station had average annual correlations of $r = 0.95+/-0.01$. $\Delta T_{a850}$, $ZW_{850}$ and $MW_{850}$ showed statistically significant differences in distribution ($p < 0.0001$; $n > 5000$), however plots of the cumulative frequency distribution for $\Delta T_{a850}$ and $MW_{850}$ showed little divergence between the release points

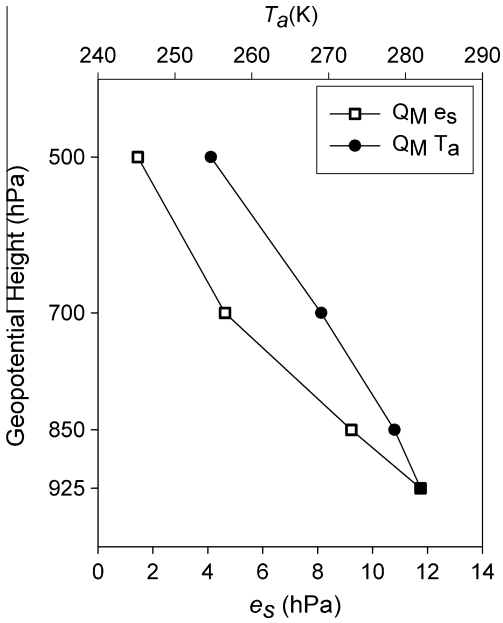


**Fig. 3.** Average atmospheric boundary layer meteorological profiles for $T_a$ and *es* associated with high magnitude melt ($Q_M$) events at Site 1 during the 2007 ablation season.

(Fig. 5), and the Pettit test indicated that a change point coincident with the station move did not occur in the time-series of these two parameters. However, a significant difference was detected for $ZW_{850}$, as both statistical tests and the cumulative distribution frequency plots indicated that a change point in the data occurred in 1994. To account for this, the Vernon radiosonde record was adjusted by the difference in median $ZW_{850}$ ($-0.7$ m s$^{-1}$) between the two release points. Subsequent tests indicated that there was no significant difference in distribution or variance for the adjusted $ZW_{850}$ data, the change point had shifted to 1984, and the distributions were more closely matched (Fig. 5).

Table 3 shows correlations between $Q'_{M1}$ and $Q'_{M2}$, and regional discharge and snowmelt records. There is little difference in correlation strength following the radiosonde station move, indicating that the ability of the derived melt indices to represent regional variability of melt events was unaffected by the move.

The derivation of equations from a single year of field data required that the 2007 radiosonde data be compared to the long-term record (1972–2012) to determine whether 2007 could be considered "representative" of the radiosonde record in its entirety. Cumulative frequency distributions of the predictor variables were compared for March–May in 2007 and the same months for 1972–2006 and 2008–2012 (Fig. 6), and significant differences in distributions were tested for using the Kolmogorov–Smirnov test. With the exception of $\Delta T_{a850}$ ($p = 0.03$) and $MW_{850}$ ($p = 0.04$), there was no significant difference in medians between 2007 and the rest of the record period, and only $MW_{850}$ showed a significant difference in variance ($p = 0.001$). Given the close correspondence between the cumulative frequency distributions, and that the dominant predictor variables ($T_{a850}$ and $e_{s850}$) were not significantly different between the two periods, the ablation season of 2007 can be considered representative of the other years analysed.

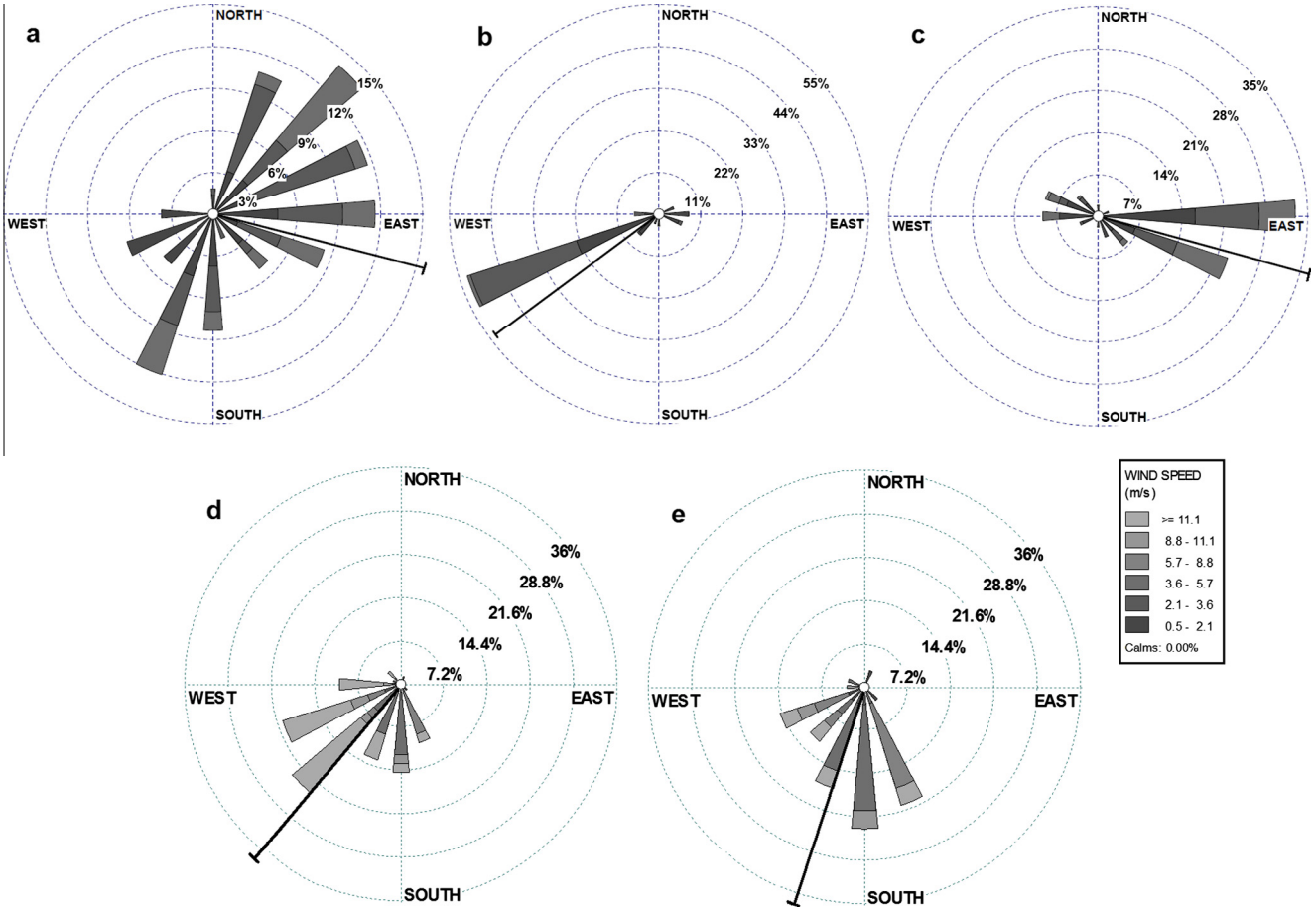


**Fig. 4.** Wind roses for high magnitude melt events (>10 mm d$^{-1}$) for (a) Site 1 (1450 masl), (b) Site 2 (980 masl), (c) Coldstream Ranch climate station (482 masl), (d) 700 hPa geopotential height (~3000 masl) and (e) 850 hPa (~1400 masl).

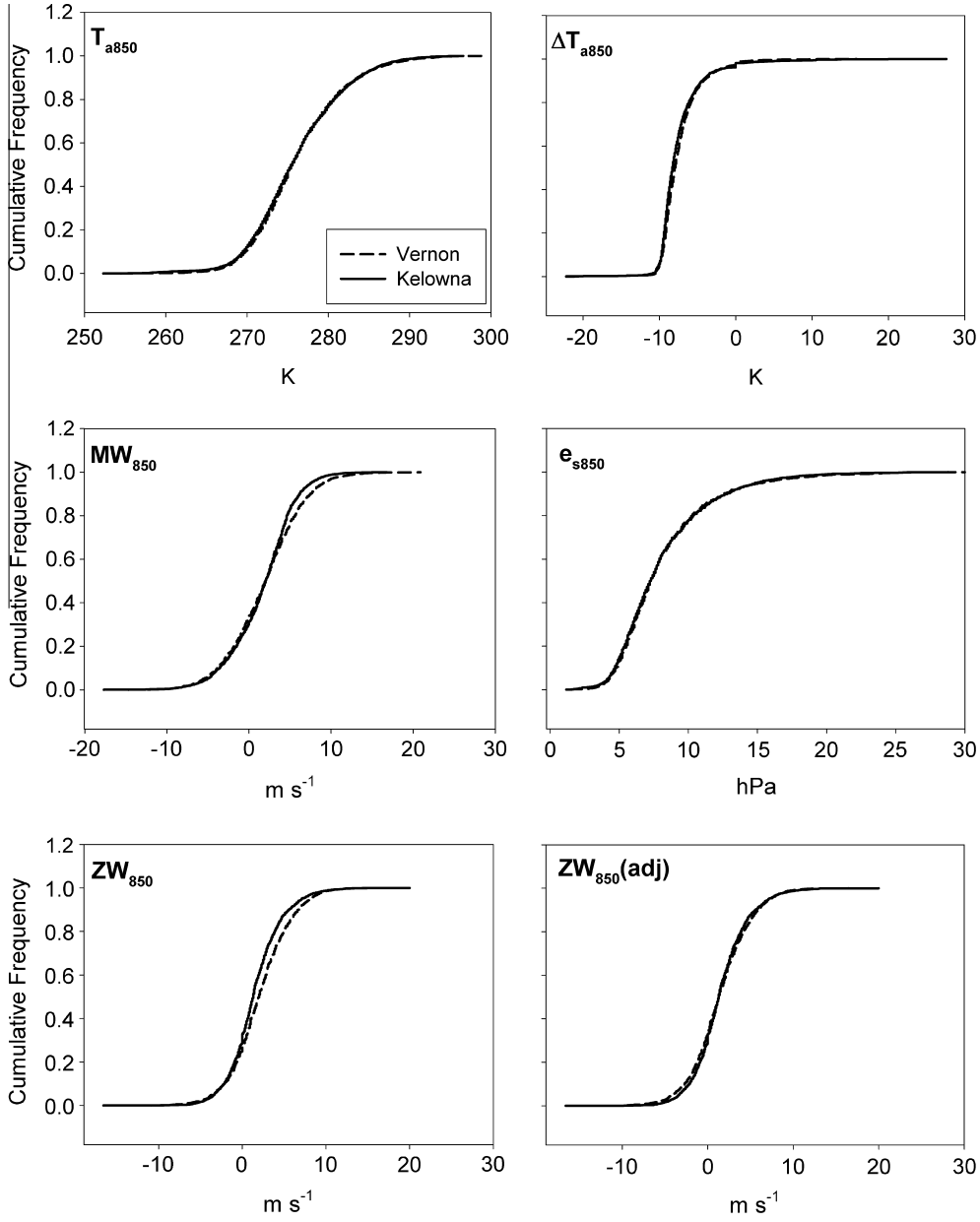


**Fig. 5.** Cumulative frequency distributions for parameters measured by radiosonde flights from Vernon (1972–1993) and Kelowna (1994–2012).

**Table 3**
Pearson's correlation coefficients ($r$) for melt values calculated using the multiple linear regression model compared to discharge in Coldstream Creek (_Q) and snowmelt at the Park Mountain (1F03P) and Mission Creek 2F05P snow pillows. Values shown are average correlations for the periods indicated, corresponding to the change in radiosonde release location in 1994.

| | | Coldstream_Q | 1F03P | 2F05P |
|---|---|---|---|---|
| Site 1 | 1972–1993 | 0.61 | 0.62 | 0.47 |
| | 1994–2011 | 0.62 | 0.59 | 0.45 |
| Site 2 | 1972–1993 | 0.65 | 0.65 | 0.49 |
| | 1994–2011 | 0.67 | 0.61 | 0.47 |

### 3.2. Snow melt models

Linear regression models were constructed using the 850 hPa data to assess the variance in snowmelt ($Q_M$) at the two field sites (Site 1 and 2) from the ablation season of 2007, and these models were then used to predict $Q_M$ ($Q'_M$) for the radiosonde period of record (1972–2012). Hourly surface measurements of snow melt from the SNTHERM outputs (Jackson and Prowse, 2009) were aggregated for 12-h periods centred on the radiosonde flight times (00 and 12 UTC).

The variables assessed for inclusion in the model were (see Appendix A): $Z_{850}$, $T_{a850}$, $\Delta T_{a850}$, $e_{850}$, $e_{s850}$, $U_{850}$, $ZW_{850}$, $MW_{850}$, and $K^*$ (Fig. 2). These variables were the most highly correlated with melt, and are the required inputs to most physically based snowmelt models, along with radiation. Analyses using only the ABL data as predictors produced residuals with marked heteroscedasticity, indicating that the models ability to predict $Q_M$ deteriorated later in the ablation season when the largest events occurred, concurrent with the increasing contribution of shortwave radiation to the snow energy balance (Jackson and Prowse, 2009). Since incident shortwave radiation is not measured by radiosonde flights, the clear sky solar radiation ($K^*$) was used as a surrogate; calculated following Bird and Hulstrom (1981). This model is based on empirical interpretations of radiative

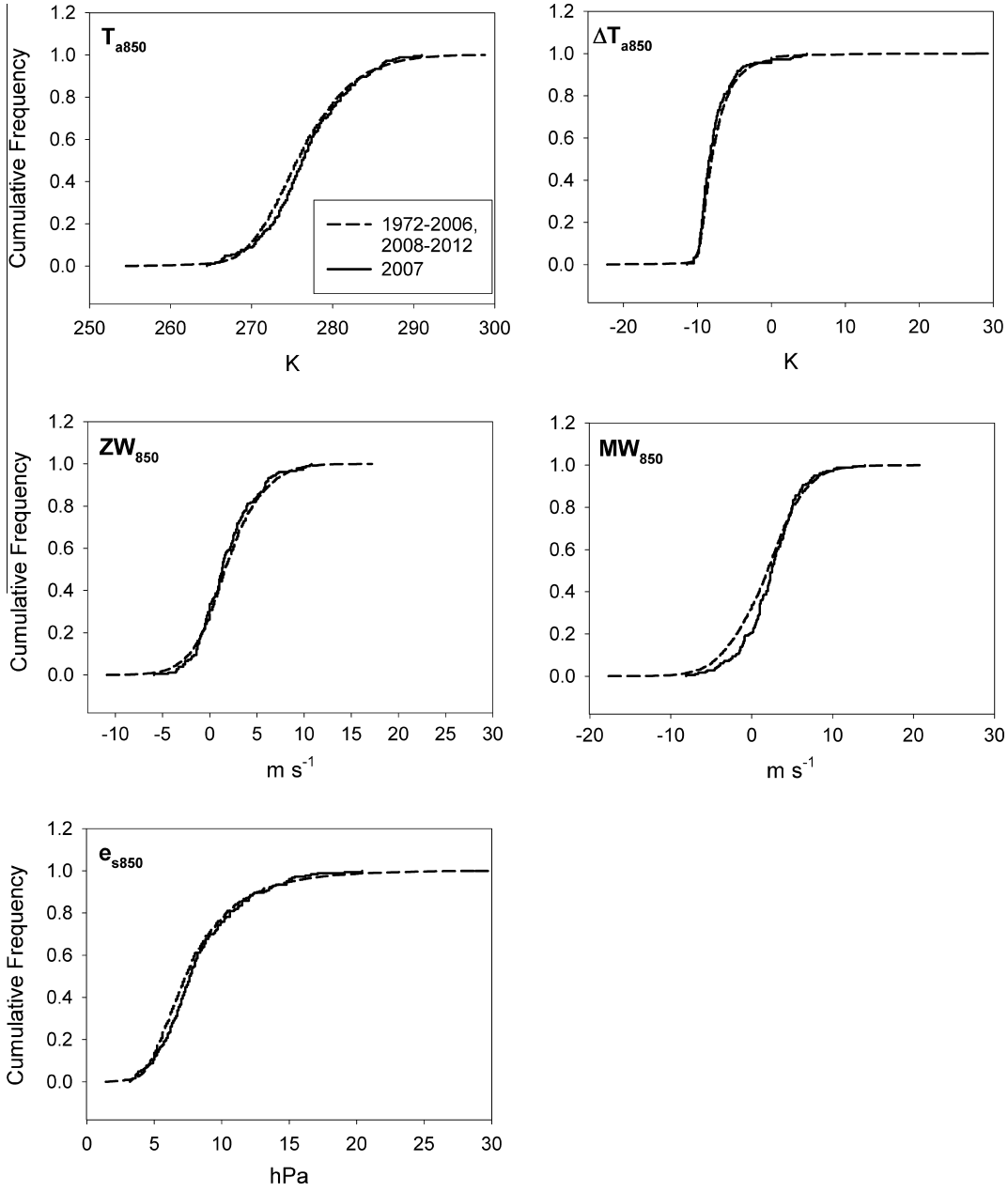


**Fig. 6.** Comparison of cumulative frequency distributions for parameters measured by radiosonde flights from 2007 and 1972–2006, 2008–2012.

transmittance and absorption by atmospheric constituents including water vapour, ozone and atmospheric particulates. It is widely used for the estimation of broadband clear sky irradiance at the Earth's surface (e.g., Pellicciotti et al., 2011). The model provides comparable estimates of hemispherical radiation, within 10% of more complex theoretical equations, and within the error range of most pyranometers (25–100 W $m^{-2}$; Myers, 2005).

Regression models were also constructed to predict snow surface vapour exchange (i.e., evaporation, condensation and sublimation). However, the predictive ability of these equations was limited (Site 1 $R^2 = 0.31$; Site 2 $R^2 = 0.45$). Since these fluxes are one to several orders of magnitude smaller than the snow melt values, and are difficult to verify against another measured dataset, these indices were not carried forward for further analysis.

A multiple stepwise regression with forward selection process determined which combination of atmospheric boundary layer (ABL) variables measured at the 850 hPa height were best able to explain the variance in $Q_M$. All variables were retained at the 95% significance level, and autocorrelation was tested using the Durbin–Watson statistic. The melt indices for both sites were validated using daily basin streamflow and regional snow melt records for the same period of record. Note that similar analyses were also conducted using principal components regression (Garen, 1992; Jackson, 2003), and non-linear regression techniques (not shown) but the predictive skill was not an improvement on the multiple regression results.

The models below provide indices for melt at Site 1 ($Q'_{M1}$) and at Site 2 ($Q'_{M2}$) throughout this study. The units for all variables are listed in Appendix A.

$$Q'_{M1} = 326.627 - 1.304T_{a850} - 0.142\Delta T_{a850} + 4.31e_{s850} - 0.166ZW_{850} + 0.403MW_{850} + 0.009K^{*} \quad (1)$$

$$Q'_{M2} = 475.72 - 1.879T_{a850} + 5.991e_{s850} + 0.01K^{*} \quad (2)$$

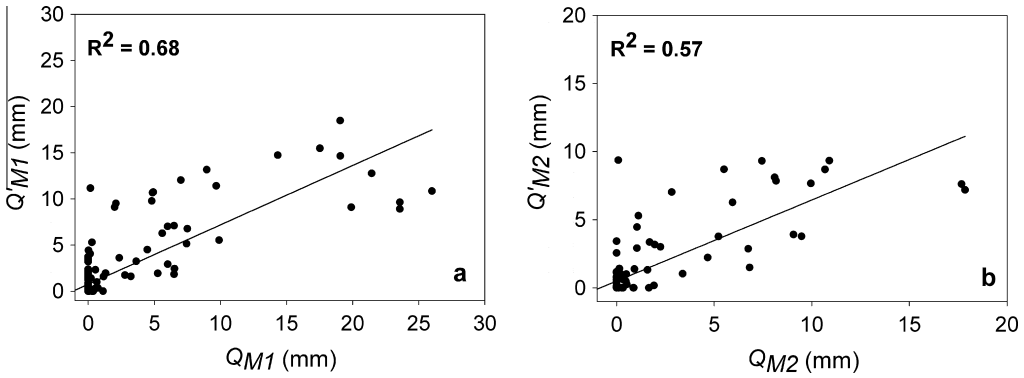


**Fig. 7.** Observed ($Q_M$) vs. predicted ($Q'_M$) melt from multiple regression model for (a) Site 1 and (b), Site 2 for Julian Day 44–109, 2007.

$Q'_{M1}$ explained 68% of the variance in measured melt (RMSE = 5.8 mm), and $Q'_{M2}$ explained 57% of the variance in melt rates (RMSE = 8.2 mm; Fig. 7).

$Q'_{M1}$ includes both zonal wind and meridional wind components as predictor variables, but $Q''_{M2}$ does not. Jackson and Prowse (2009) found that the majority of high magnitude melt events at Site 2 were driven by radiation inputs, while melt events at Site 1 were driven more by sensible heat fluxes, and this difference is reflected in the retained predictor variables for each site. The inclusion of both zonal and meridional wind variables in $Q'_{M1}$ accounts for the bimodal distribution of winds at this site (Fig. 4), with a higher weight placed on the synoptic scale winds (meridional in this case), which comprised the dominant wind direction noted for high magnitude melt events in the 2007 ablation season. Therefore the equations are considered to accurately represent the synoptic drivers of melt in the Coldstream Basin.

### 3.3. Verification of modelled melt indices

$Q_{M1}$, $Q_{M2}$, $Q'_{M1}$ and $Q''_{M2}$ were significantly correlated with discharge measured at the Coldstream Creek gauge at a two day lag in 2007. $Q_M$ at both sites showed modest correlations with streamflow in 2007 (Site 1 $r = 0.51$; Site 2 $r = 0.52$), however, $Q'_M$ had a stronger relationship (Site 1 $r = 0.63$; Site 2 $r = 0.67$) with streamflow than $Q_M$ values obtained from site specific measurements (Jackson and Prowse, 2009). This indicates that $Q'_M$ better represents the temporal variation in basin-wide snowmelt than the site-specific values. Since point scale snow energy balance is a function of synoptic conditions, modified by local topography and vegetation, these results highlight the utility of upper air data for estimating snowmelt at the basin scale. Fig. 8 shows the relationship between $Q'_M$ for Sites 1 and 2 with streamflow in Coldstream Creek for the freshets of 1982 (high discharge), 2005 (low discharge), and 2007 (representative year). The timing of large melt events estimated from the radiosonde record coincides very closely with rises in streamflow, and highlights the strong nival control on streamflow in this basin. Note that the estimated melt is not included after Julian Day 125 in 2005 and 2007, as the snowpack has been depleted by this point. $Q'_{M1}$ correlations with streamflow were $r = 0.64$ over the full record period, while $Q''_{M2}$ had an average annual correlation of $r = 0.67$ (Table 4 and Fig. 9).

Similar results were obtained from comparisons between $Q'_{M1}$ and $Q'_{M2}$ and daily melt measured at the nearby Park Mountain and Mission Creek snow pillows (Table 4 and Fig. 9). The median annual RMSE between melt calculated from the ABL data and regional melt values ranged from 13 to 21 mm, and median annual correlations ranged from 0.37 to 0.68 (between sites). In general, RMSE was relatively consistent for all sites, and slightly higher for site specific values of $Q_M$ and $Q'_M$. Both snow pillows are located

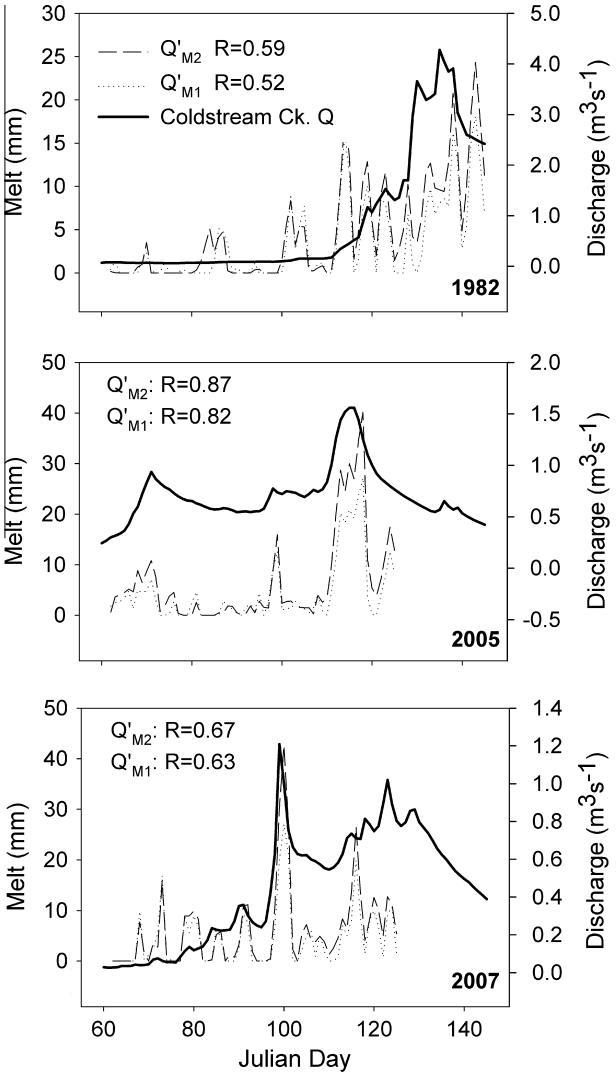


**Fig. 8.** $Q'_M$ calculated from ABL conditions for Sites 1 and 2 plotted with streamflow measured at Coldstream Creek above the Municipal Intake (08NM142), for the years 1982, 2005 and 2007.

at higher elevations than the Coldstream sites (Table 1), therefore the melt estimates derived for the Coldstream sites are expected to be higher, and would show the melt season starting and ending earlier than it would at the snow pillows. No corrections for the difference in elevation (ranging from 338 to 877 m) were made before calculating the RMSE.

**Table 4**
Median correlations and RMSE (melt only) between melt indices calculated for Sites 1 and 2, streamflow in Coldstream Creek (08NM142), and snow melt measured at the Park Mountain (1F03P) and Mission Creek (2F05P) snow pillows. RMSE values in brackets are standard deviation for the annual RMSE. Melt estimates were not adjusted for elevation differences between the study sites and the snow pillows prior to calculating the RMSE.

| | | Site 1 | Site 2 |
|---|---|---|---|
| 08NM142 | *r* | 0.64 | 0.67 |
| 1F03P | RMSE | 13.5 (4.3) | 20.6 (6.1) |
| | *r* | 0.60 | 0.61 |
| 2F05P | RMSE | 12.9 (4.9) | 19.2 (6.7) |
| | *r* | 0.46 | 0.49 |

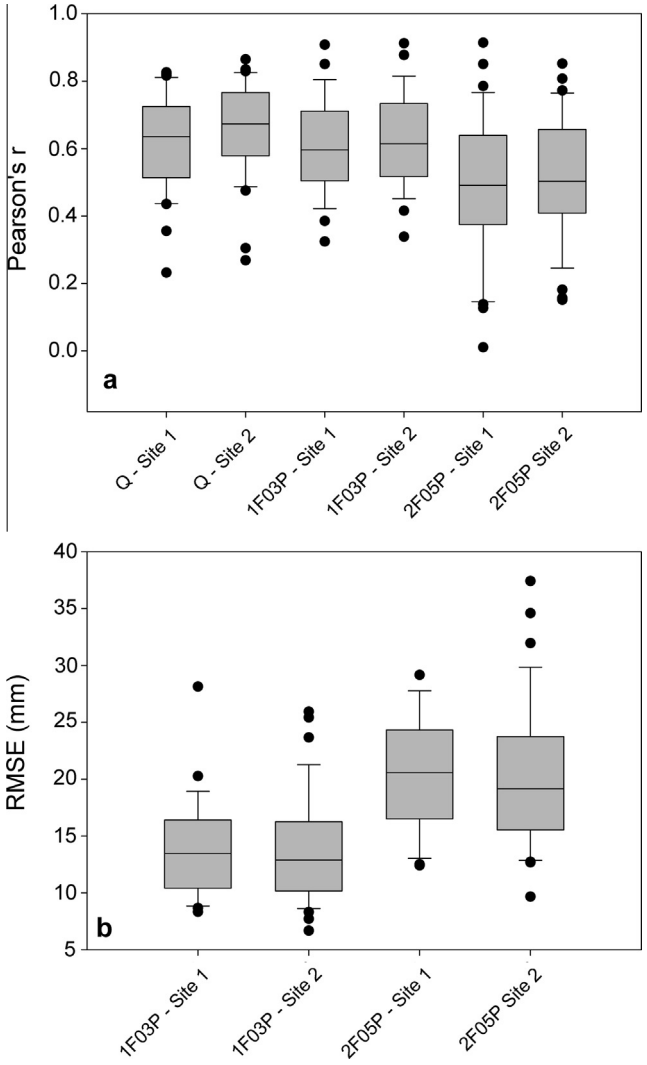


**Fig. 9.** Annual correlations (a) between melt indices for Sites 1 and 2 and streamflow ($Q$; $n = 34$), melt at the Park Mountain (1F03P; $n = 23$) and Mission Creek snow pillows (2F05P; $n = 34$), and (b) RMSE for calculated melt indices and measured melt at the same snow pillows.

Correlations were higher between $Q'_M$ and Park Mountain snow pillow data than Mission Creek snow pillow data. Relative proximity of these stations to the field sites (34 km and 45 km, respectively) and site characteristics support this result. The Park Mountain station, situated in a large opening near treeline, is more similar to the field sites in the Coldstream basin than the Mission Creek station, which is located in a small opening in mature forest. Therefore, based on the high degree of correspondence between $Q'_M$ and the regional data, the derived indices were considered to be representative of ablation season snow surface energy processes at the basin scale.

### 3.4. Ablation season trends and teleconnection linkages

The study period (1972–2012) is marked by pronounced large-scale climatic changes, including rising temperatures both globally and regionally, the well documented phase shift of the *PDO* in 1976/77, and increased frequency and magnitude of El Niño events (Lemke et al., 2007). To determine if similar changes occurred in the study basin, temperature and precipitation, the predictor variables from the radiosonde data, derived melt indices, April 1st SWE values, and date of freshet initiation (calculated following Cayan et al., 2001) were tested for significant trends over the period 1972–2010, as not all data sets were current to 2012 at the time of writing (Table 5). Long term monthly temperature and precipitation records for the Vernon climate station were downloaded from the Adjusted and Homogenized Canadian Climate Data (AHCCD; Environment Canada, 2012a) archive (1900–2011, Table 1). Streamflow data for the outlet of the Coldstream basin were taken from the Coldstream Creek above the Municipal Intake station (WSC 08NM142).

The traditional March–April–May (MAM) spring period was used to provide a consistent reference ablation season that was not subject to seasonal temperature changes over time. An annual series of high-magnitude melt events was constructed (defined as $>1\sigma$ above the record period average $Q'_M$), and the number of $>1\sigma$ $Q'_M$ events, number of $>1\sigma$ $Q'_M$ events of two or more days, and length of longest sequent $>1\sigma$ $Q'_M$ events were also documented. The latter two variables were included as measures of the frequency and duration of large melt events in a given year. Data were pre-whitened (Yue et al., 2002) prior to applying the Mann–Kendall trend test (Mann, 1945; Kendall, 1975) with Sen's slope analysis (Bronaugh and Werner, 2008).

The El Niño Southern Oscillation (*ENSO*), and the Pacific Decadal Oscillation (*PDO*) (Mantua et al., 1997; source: http://jisao.washington.edu/pdo/PDO.latest) are the two main teleconnections that exert a strong influence on annual snowpack fluctuations in western North America. The *MEI* (Multi-variate El Niño Index) (Wolter and Timlin, 1993); source: http://www.esrl.noaa.gov/psd/enso/mei/table.html) is considered to be a more robust index of the *ENSO* than the traditional Southern Oscillation Index (SOI), and is used here (Wolter and Timlin, 1998). The Multivariate *ENSO* Index was used for this analysis since it represents several atmosphere–ocean related components in the tropical Pacific, while the traditional SOI and Nino 3.4 indices only quantify atmospheric (SOI) or sea-surface temperature (Nino 3.4) conditions. Several studies have shown a strong relationship amongst these *ENSO* indices (e.g., Kiem and Franks, 2001; Hanley et al., 2003; Wolter and Timlin, 2011), therefore, the findings from this analysis would not be changed with the choice of a different index.

To assess the relationships between the *ENSO* and *PDO* and the calculated melt indices, correlations were calculated using the Pearson's correlation coefficient ($r$) for the standard climatological winter – December–January–February (DJF); and spring periods – (MAM). The former allows for potential climatic lag effects while the latter comprises the ablation season in the Okanagan Basin. The effects of the *ENSO* and *PDO* indices on observed hydroclimatic trends and variability were examined using a two stage trend detection process. First, the melt indices showing significant trends were regressed against all significantly correlated teleconnection indices using multiple stepwise regression. Second, the residuals of the regression equations that explained a significant proportion of the annual variation with the *ENSO* and *PDO* were tested again for trends to assess whether the trend was statistically

**Table 5**
Variables tested for trends and correlations with teleconnection indices. Note: $\langle\chi\rangle$ denotes average, $\sigma$ denotes standard deviation.

| March–April–May (for Sites 1 and 2) | | SWE and discharge |
|---|---|---|
| *Values derived from regression estimates* | | |
| *MAX* $Q'_M$ | | *MAX Q* |
| $\langle Q'_M\rangle$ | | $\langle Q\rangle$ |
| $\sigma Q'_M$ | | *MAX Q date* |
| # days >1$\sigma$ $Q'_M$ | | April 1st SWE |
| # events >1$\sigma$ $Q'_M$ of >=2 days | | Date of snowmelt initiation |
| Length of longest sequent period >1$\sigma$ $Q'_M$ | | Date of freshet initiation |
| *Values from radiosonde record – 850 hPa geopotential height* | | *1200 and 2400 UTC readings* |
| $\langle T_{a850}\rangle$ | *MAX* $T_{a850}$ | $\sigma$ $T_{a850}$ |
| $\langle \Delta T_{a850}\rangle$ | *MAX* $\Delta T_{a850}$ | $\sigma$ $\Delta T_{a850}$ |
| $\langle e_{s850}\rangle$ | *MAX* $e_{s850}$ | $\sigma$ $e_{s850}$ |
| $\langle ZW_{850}\rangle$ | *MAX* $ZW_{850}$ | $\sigma$ $ZW_{850}$ |
| $\langle MW_{850}\rangle$ | *MAX* $MW_{850}$ | $\sigma$ $MW_{850}$ |

independent of the influential teleconnection indices. The intention was to determine whether the unexplained portion still exhibited a trend that was not a result of the positive phase of the *PDO* that spans a large portion of the record period, or increases in *ENSO* magnitude over time, for example.

## 4. Results and discussion

### 4.1. Hydroclimatic trends and teleconnection linkages

Significant, positive trends were found for winter and spring maximum monthly temperatures at the Vernon climate station over the 1972–2010 period (Table 6). The trend magnitude was higher for winter temperature than for spring (~0.6° decade$^{-1}$ and 0.4° decade$^{-1}$, respectively; $p < 0.10$,), indicating that winter temperatures are rising faster than spring temperatures over the last few decades in the northern Okanagan. Maximum temperature was the only winter season variable significantly correlated to a teleconnection index (DJF *PDO*), while all spring temperature variables had significant positive correlations with the winter and spring *MEI* and *PDO* indices. As a result of the increasing winter and spring temperatures, the date of snowmelt initiation is shifting earlier in the year by 2.5 days decade$^{-1}$ ($p = 0.27$). and is significantly correlated with the winter and spring *MEI* (Table 6).

Spring and summer total precipitation is decreasing at ~8 mm and 6 mm decade$^{-1}$ (respectively), but only the former trend is significant. Correlations with the *MEI* and *PDO* indices are generally weak and not significant, except summer precipitation, which is significantly negatively correlated with the preceding winters *PDO* and *MEI* phase (Table 6). It is noteworthy that over the period 1900–2010, the trends for spring and summer precipitation are positive (~1.5 mm decade$^{-1}$), which indicates that the direction and magnitude of the trend is at least partly dependent on the period analysed.

Significant positive trends were found in the 1200 UTC radiosonde data for the maximum and standard deviation of the vertical air temperature gradient at the 850 hPa height (1.5 °C decade$^{-1}$ and 0.2 °C decade$^{-1}$, respectively). A similar trend was found for the latter variable from the 2400 UTC flight (0.1 °C decade$^{-1}$). Neither variable was significantly correlated with the *MEI* or *PDO*. The average gradient from the 1200 UTC flight was positively correlated with the winter and spring *MEI*, and showed a slight positive trend (0.1 °C decade$^{-1}$) for the 2400 UTC reading, but no significant correlations with the *MEI* or *PDO* (Table 6). These results indicate that the upper end of the vertical temperature gradient in the atmospheric boundary layer has increased over the period 1972–2010, as has the seasonal variability in the gradient.

Average $T_a$ and $e_s$ at the 850 hPa height (1200 and 2400 UTC flights) were strongly positively correlated with the winter and spring *MEI* and *PDO* indices, but showed no significant trends (Table 6). These results indicate that positive (warm) phases of these teleconnections are associated with warmer synoptic scale air temperatures and higher atmospheric moisture content. The winter *PDO* had a relatively lower correlation with the variables measured at the 850 hPa height than the other indices, similar to the results for temperature from the Vernon AHCCD record. Maximum $T_a$ (2400 UTC), however, showed a slight positive trend (0.6 °C decade$^{-1}$), and was correlated with the DJF *PDO*. The trend direction and magnitude remained constant after considering the potential influence of the *PDO* (Table 6).

A negative but not significant (−17 mm decade$^{-1}$), trend was found for April 1st SWE values at the Silver Star snow course (2F10; Table 7). Significant negative correlations exist between April 1st SWE and the winter and spring *MEI* and *PDO*, indicating that warm (cool) phases of both teleconnections are linked to reduced (increased) spring snowpacks in the northern Okanagan Basin. Previous studies examining snowpack and teleconnection linkages in British Columbia and the western USA have found that

**Table 6**
Significant trends and teleconnection correlations for regional hydroclimatic parameters for the period 1972–2010. Refer to Appendix A for variable descriptions.

| Variable | Trend yr$^{-1}$ | MEI_DJF | MEI_MAM | PDO_DJF | PDO_MAM |
|---|---|---|---|---|---|
| *Regional temperature, precipitation, and vapour pressure* | | | | | |
| Winter max$T_a$[a] | *0.057* | 0.19 | 0.15 | *0.31* | 0.21 |
| Spring min$T_a$ | 0.002 | **0.53** | **0.41** | **0.53** | **0.53** |
| Spring $\langle T_a\rangle$ | 0.023 | **0.61** | **0.53** | **0.49** | **0.55** |
| Spring max$T_a$[a] | *0.036* | **0.60** | **0.55** | **0.39** | **0.49** |
| Spr_Isotherm | −0.250 | **−0.45** | **−0.35** | −0.24 | −0.28 |
| Spring precip. | *−0.875* | −0.12 | −0.11 | 0.01 | 0.25 |
| Summer precip. | −0.612 | **−0.35** | −0.08 | **−0.42** | −0.28 |
| *March–April–May radiosonde data – 1200 UTC readings* | | | | | |
| $\langle T_{a850}\rangle$ | 0.009 | **0.59** | **0.59** | **0.45** | **0.59** |
| *MAX* $\Delta T_{a850}$ | **0.145** | −0.10 | −0.13 | 0.10 | 0.04 |
| $\langle \Delta T_{a850}\rangle$ | −0.003 | **0.44** | **0.37** | 0.25 | **0.43** |
| $\sigma$ $\Delta T_{a850}$ | **0.020** | −0.11 | −0.14 | 0.09 | 0.01 |
| $\langle e_{s850}\rangle$ | 0.005 | **0.56** | **0.64** | **0.44** | **0.56** |
| *March–April–May radiosonde data – 2400 UTC readings* | | | | | |
| $\langle T_{a850}\rangle$ | 0.015 | **0.64** | **0.61** | **0.46** | **0.65** |
| *MAX* $T_{a850}$[a] | *0.062* | 0.24 | 0.27 | *0.31* | 0.10 |
| $\langle \Delta T_{a850}\rangle$ | **−0.011** | −0.06 | 0.03 | 0.11 | 0.18 |
| $\sigma$ $\Delta T_{a850}$ | *0.013* | −0.13 | −0.01 | −0.02 | 0.01 |
| $\langle e_{s850}\rangle$ | 0.010 | **0.63** | **0.68** | **0.45** | **0.60** |

Values in bold are significant at $p < 0.05$, values in italics are significant at $p < 0.10$, and values denoted by * are significant at $p < 0.15$. $\langle x\rangle$ refers to average, and $\sigma$ refers to standard deviation. Only those variables with a significant trend or two or more significant correlations with a teleconnection index are shown.

[a] Trend calculated on the residuals remaining after the influence of the relevant teleconnections on the original time-series has been taken into account.

**Table 7**
Significant trends and teleconnection correlations for regional snowmelt and discharge, and snowmelt estimates derived from the radiosonde record, for the period 1972–2010. Format is the same as for Table 6.

| Variable | Trend $yr^{-1}$ | MEI_DJF | MEI_MAM | PDO_DJF | PDO_MAM |
|---|---|---|---|---|---|
| *Snowmelt and discharge* | | | | | |
| MAX 2F10 SWE | −1.719 | **−0.49** | **−0.41** | **−0.54** | **−0.48** |
| MAX Q date | −0.214 | **−0.45** | **−0.36** | −0.22 | *−0.33* |
| Pulse date[a] | **−0.447** | **−0.64** | **−0.57** | **−0.39** | **−0.56** |
| *Melt Indices – Site 1* | | | | | |
| $\langle Q'_{M1} \rangle$ | 0.042 | **0.52** | **0.68** | **0.43** | **0.52** |
| $\sigma Q'_{M1}$ | 0.032 | 0.21 | **0.42** | *0.31* | 0.21 |
| #>+1σ[b] | 0.063 | **0.46** | **0.62** | *0.30* | *0.34* |
| Largest event[c] | No trend | **0.35** | **0.42** | *0.30* | 0.20 |
| *Melt indices – Site 2* | | | | | |
| $\langle Q'_{M2} \rangle$ | 0.063 | **0.55** | **0.70** | **0.41** | **0.51** |
| $\sigma Q'_{M2}$ | 0.060 | 0.22 | **0.41** | *0.30* | 0.22 |
| #>+1σ[b] | 0.086 | **0.48** | **0.65** | *0.33* | *0.33* |
| Largest event[c] | No trend | **0.43** | **0.46** | *0.31* | 0.27 |

[a] Trend calculated on the residuals remaining after the influence of the relevant teleconnections on the original time-series has been taken into account.
[b] Number of melt events greater than one standard deviation above the long-term mean.
[c] Number of consecutive days with $Q'_M$ greater than one standard deviation above the long-term mean.

warm (positive) phases of the *PDO* and *ENSO* indices result in higher than average winter and spring temperatures, lower than average precipitation and therefore, below average April 1st SWE. These effects are magnified when one or more of these indices are in phase (e.g., Hsieh and Tang, 2001; Stahl et al., 2006).

### 4.2. Snowmelt and discharge trends and teleconnection linkages

Significant trends were found towards earlier dates of freshet initiation (5.0 days $decade^{-1}$) and peak freshet discharge (2.1 days $decade^{-1}$; Table 7) over the period 1972–2010; similar to those identified by Zhang et al., 2001 and Stewart et al., 2005. As with all trends identified in this analysis, there was substantial inter-annual variability around the trend line. Positive (negative) phases of the *PDO* and *MEI* are characterised by warmer (cooler) than average $T_a$, which are correlated with a significantly earlier (later) onset of the freshet. The winter *MEI* was the strongest predictor for both streamflow timing measures, while the retained trend (using the residuals from the regression between winter and spring *MEI* and freshet initiation) showed the trend towards earlier freshet initiation moderating somewhat (4.5 days $decade^{-1}$; $p = 0.009$). No significant trend was noted for the maximum annual discharge in Coldstream Creek. These results suggest that even though the *MEI* is linked to the timing of streamflow in the Coldstream basin, it does not alter the underlying trend towards earlier freshet initiation and peak flow.

Average melt indices ($Q'_M$) for Sites 1 and 2 were positively correlated with the winter and spring *MEI* and *PDO*. The same is true for the number of days in a melt season with melt rates greater than one standard deviation above the long-term mean (#>+1$\sigma$), and the length of the longest duration melt event. The standard deviation of the melt indices at both sites was positively correlated with the spring *MEI* and winter *PDO* (Table 7). No significant trends were found for any of the melt indices, indicating that while the magnitude, duration and variability of melt events is influenced by the *MEI* and *PDO*, these metrics are not changing appreciably over time.

In summary, the results of the analyses presented here show that the hydroclimatic regime of the northern Okanagan Basin, and the Coldstream basin in particular, is experiencing significant changes in the amount of warm season precipitation, snow accumulation, vertical temperature gradients in the atmospheric boundary layer, and the streamflow generated by these processes. Warm season precipitation in the northern Okanagan is decreasing over the period studied, and snowpacks at higher elevations are decreasing due to higher spring temperatures. The beginning of the ablation season is moving earlier in the year, concurrent with an earlier start to the freshet, and an earlier peak freshet discharge. Positive (warm) phases of the *ENSO* and *PDO* are significantly correlated with increased melt rates, resulting from higher air temperature and saturated vapour pressure measured at the 850 hPa height during these phases. The trends found in this analysis remain similar, regardless of the *ENSO* or *PDO* phase. These results have significant implications for storage of melt water within reservoirs and groundwater, increases the potential for snowmelt driven flood events, and will result in reductions to the volume of water available for maintenance of summer low flows.

## 5. Conclusions

This work has quantified the linkages between micro-scale snow surface processes and the associated conditions in the ABL, identified trends in hydroclimatic parameters and clarified the connections to the dominant teleconnection patterns influencing climate in the Okanagan Basin, British Columbia. Statistical models based on radiosonde data were found to be good predictors of the measured variation in melt rates in the Coldstream Basin, and the larger northern Okanagan. These models formed the basis for historical estimates of melt, which were subsequently correlated with well-known, large-scale teleconnection indices. Significant trends were noted towards higher winter and spring temperatures, and earlier dates of snowmelt and freshet initiation. The frequency and duration of high magnitude melt events did not show significant trends. Significant positive correlations were found between the primary atmospheric parameters that influence snowmelt, including spring air temperature, the melt indices derived from these parameters, and the positive phases of the spring and winter *ENSO* and *PDO*. If current trends continue in the Okanagan Basin, the onset of the snowmelt period and the resulting streamflows will occur earlier in the year, and more rapidly, particularly during positive phases of the *ENSO* and *PDO*. These results are in agreement with similar studies conducted in western North America.

Where radiosonde records exist, the data contained within them has the potential to better represent the climatic conditions over a larger basin scale than site-specific measurements would (e.g., Lundquist et al., 2010). Due to the operational requirements for radiosonde data, the records are generally complete, have long record periods, and measure variables not typically measured by

ground climate stations. Therefore, these data sets provide a unique opportunity to assess snowmelt (and likely other components of the hydrological cycle) over broader spatial and temporal scales than would be possible using only ground based climate stations. The methods presented here show promise for wider application, particularly where site-specific data are lacking, or where site data are heavily influenced by the surrounding topography and vegetation, and are thus not easily scaled to dissimilar areas within the same basin. Because these data are more representative of the synoptic conditions in the ABL, they can be more useful for large scale assessments of snow energy balance than site specific measurements.

However, for the same reason, melt rates calculated from radiosonde data are not reflective of the influence of site-specific factors such as vegetation or topography, and require a data-set to 'ground truth' the estimates against. In order to link the radiosonde measurements with the basin scale hydrological response, more micro-meteorological measurement points within the basin would be required to appropriately scale atmospheric conditions over the entire basin. This would also allow the issue of bias between the radiosonde measurements and those taken at the site scale to be addressed, and is an area of focus for future research.

While the work presented here elucidates the linkages between conditions in the ABL and those at the snow surface, the linkages between the meso-scale synoptic conditions and the ABL are still undefined. Future studies should seek to describe the links between the synoptic conditions associated with high magnitude melt events and the phase and strength of the various teleconnections that drive snowmelt in the Okanagan Basin. This requires a long term high-elevation monitoring program, with several sites distributed along the north–south precipitation gradient in the Okanagan Basin.

## Acknowledgements

The authors gratefully acknowledge the funding support for this work provided by the Natural Science and Engineering Research Council (NSERC), the Water and Climate Impacts Research Centre (W-CIRC), Environment Canada and the University of Victoria. Thanks also to Trevor Semchuck and Tom Carter for assistance in the field, and to William Floyd for the productive insights into change point analysis. Figure 1 was created by Ole Heggen. Three anonymous reviewers provided comments that contributed substantially to the improvement of this manuscript.

## Appendix A. Abbreviations

| Abbreviation | Description | Units |
|---|---|---|
| $Q_M$ | Melt | mm day$^{-1}$ |
| $Q'_M$ | Melt index | mm day$^{-1}$ |
| $Q_{M1}$ | Coldstream Up (Site 1) measured melt | mm day$^{-1}$ |
| $Q'_{M1}$ | Coldstream Up (Site 1) melt index | mm day$^{-1}$ |
| $Q_{M2}$ | Coldstream Mid (Site 2) measured melt | mm day$^{-1}$ |
| $Q'_{M2}$ | Coldstream Mid (Site 2) melt index | mm day$^{-1}$ |
| $Z_{850}$ | 850 hPa geopotential height | masl |
| $\Delta T_{a850}$ | 850 hPa temperature gradient | K km$^{-1}$ |
| $ZW_{850}$ | 850 hPa zonal wind | m s$^{-1}$ |
| $MW_{850}$ | 850 hPa meridional wind | m s$^{-1}$ |
| $U_{850}$ | 850 hPa wind speed | m s$^{-1}$ |
| $DD_{850}$ | 850 hPa dewpoint depression | K |
| $T_a$ | Air temperature | K |
| $R_n$ | Net radiation | W m$^{-2}$ |
| $K^*$ | Total clear sky short wave radiation | W m$^{-2}$ |
| $e$ | Vapour pressure | kPa |
| $e_s$ | Saturated vapour pressure | kPa |
| $U$ | Wind speed | m s$^{-1}$ |
| $H_L$ | Snow surface latent heat flux | W m$^{-2}$ |
| $H_S$ | Snow surface sensible heat flux | W m$^{-2}$ |
| DJF | December–January–February | N/A |
| MAM | March–April–May | N/A |
| *PDO* | Pacific Decadal Oscillation | Dimensionless |
| *MEI* | Multivariate ENSO index | Dimensionless |

## References

Adam, J.C., Hamlet, A.F., Lettenmaier, D.P., 2009. Implications of global climate change for snowmelt hydrology in the twenty-first century. Hydrol. Proc. 23, 962–972.

Bao, Z., Kelly, R., Wu, R., 2011. Variability of regional snow cover in spring over Western Canada and its relationship to temperature and circulation anomalies. J. Clim. 31, 1280–1294.

Barnett, T.P., Adam, J.C., Lettenmaier, D.P., 2005. Potential impacts of a warming climate on water availability in snow-dominated regions. Nature 438, 303–309.

Bavay, M., Lehning, M., Jonas, T., Löwe, H., 2009. Simulations of future snow cover and discharge in Alpine headwater catchments. Hydrol. Proc. 23, 95–108.

Bird, R.E., Hulstrom, R.L., 1981. A Simplified Clear Sky model for Direct and Diffuse Insolation on Horizontal Surfaces., SERI Technical Report SERI/TR-, Solar Energy Research Institute, Golden, CO. 642-761. <http://rredc.nrel.gov/solar/models/clearsky/>.

Blöschl, G., 1999. Scaling issues in snow hydrology. Hydrol. Proc. 13, 2149–2175.

Bonsal, B.R., Prowse, T.D., 2003. Trends and variability in spring and autumn 0 °C isotherm dates over Canada. Clim. Chang. 57, 341–358.

Boon, S., 2009. Snow ablation energy balance in a dead forest stand. Hydrol. Proc. 23, 2600–2610.

Bronaugh, D., Werner, A.T., 2008. The ZYP Trend R-package – The Zhang and Yue and Pilon methods of trend analysis: pre-whitening data, employing the Theil Sen trend estimator and the Mann-Kendall test of significance. Pacific Climate Impacts Consortium, University of Victoria, Victoria, BC.

Brown, R.D., Goodison, B.E., 1996. Interannual variability in reconstructed Canadian snow cover, 1915–1992. J. Clim. 9, 1299–1318.

Brown, R.D., Mote, P.W., 2009. The response of Northern Hemisphere snow cover to a changing climate. J. Clim. 22, 2124–2145.

Brutsaert, W., Kustas, W.P., 1987. Surface water vapour and momentum fluxes under unstable conditions from a rugged-complex area. J. Atmos. Sci. 44, 421–431.

Carroll, A.L., Regnière, J., Logan, J.A., Taylor, S.W., Bentz, B.J., Powell, J.A., 2006. Impacts of climate change on range expansion by the mountain pine beetle. Mountain Pine Beetle Initiative. Working Paper 2006-14. Natural Resources Canada, Canadian Forest Service, Pacific Forestry Centre. Victoria, British Columbia. 20p.

Cayan, D.R., Peterson, D.H., 1989. The influence of North Pacific Atmospheric Circulation on Streamflow in the West. Geophys. Mono. Ser. 55, 375–397.

Cayan, D.R., Kammerdiener, S.A., Dettinger, M.D., Caprio, J.M., Peterson, D.H., 2001. Changes in the onset of spring in the western United States. Bull. Am. Meteorol. Soc. 82, 399–415.

Clark, M.P., Serreze, M.C., McCabe, G.J., 2001. Historical effects of El Niño and La Niña events on the seasonal evolution of the montane snowpack in the Columbia and Colorado River Basins. Water Resour. Res. 37, 741–757.

Cohen, S., Kulkarni, T. (Eds.), 2001. Water Management and Climate Change in the Okanagan Basin. Environment Canada and University of British Columbia. Project A206, submitted to the Adaptation Liaison Office, Climate Change Action Fund, Natural Resources Canada, Ottawa, 75p.

Cohen, S. and Neale, T. (eds.) 2006. Participatory Integrated Assessment of Water Management and Climate Change in the Okanagan Basin, British Columbia. Environment Canada, University of British Columbia, Vancouver, British Columbia, 223p.

de Jong, C., Lawler, D., Essery, R., 2009. Preface – Mountain hydroclimatology and snow seasonality – perspectives on climate impacts, snow seasonality and hydrological change in mountain environments. Hydrol. Proc. 23, 955–961.
Déry, S.J., Brown, R.D., 2007. Recent Northern Hemisphere snow cover extent trends and implications for the snow-albedo feedback. Geophys. Res. Let., 34.
Déry, S.J., Stahl, K., Moore, R.D., Whitfield, P.H., Menounos, B., Burford, J.E., 2009. Detection of runoff timing changes in pluvial, nival, and glacial rivers of Western Canada. Water Resour. Res., 45.
Durack, P.J., Wijffels, S.E., Matear, R.J., 2012. Ocean salinities reveal strong global water cycle intensification during 1959–2000. Science 336, 455–458.
Durre, I., Yin, X., 2008. Enhanced radiosonde data for studies of vertical structure. Bull. Am. Meteorol. Soc. 89, 1257–1262.
Durre, I., Vose, R.S., Wuertz, D.B., 2006. Overview of the integrated global radiosonde archive. J. Clim. 19, 53–68.
Dyer, J.L., Mote, T.L., 2007. Trends in snow ablation over North America. Int. J. Climatol. 27, 739–748.
Environment Canada. 2012a. Adjusted and Homogenized Canadian Climate Data. <http://ec.gc.ca/dccha-ahccd/Default.asp?lang=En&n=B1F8423A-1>. (accessed October 2012).
Environment Canada. 2012b. Canadian Climate Normals 1971–2000. <http://climate.weatheroffice.ec.gc.ca/climate_normals/index_e.html>. (accessed October 2012).
Fritze, H., Stewart, I.T., Pebesma, E., 2011. Shifts in Western North American snowmelt runoff regimes for the recent warm decades. J. Hydrometeorol. 12, 989–1006.
Gaffen, D.J., Sargent, M.A., Habermann, R.E., Lanzante, J.R., 2000. Sensitivity of tropospheric and stratospheric temperature trends to radiosonde data quality. J. Clim. 13, 1776–1796.
Garen, D.C., 1992. Improved techniques in regression-based streamflow volume forecasting. J. Water Resour. Plan. Manage. 118, 654–670.
Granger, R.J., Male, D.H., 1978. Melting of a prairie snowpack. J. Appl. Meteorol. 17, 1833–1842.
Hamlet, A.F., Mote, P.W., Clark, M.P., Lettenmaier, D.P., 2005. Effects of temperature and precipitation variability on snowpack trends in the Western United States. J. Clim. 18, 4545–4561.
Hanley, D.E., Bourassa, M.A., O'Brien, J.J., Smith, S.R., Spade, E.R., 2003. A quantitative evaluation of ENSO indices. J. Clim. 16, 1249–1258.
Hsieh, W.W., Tang, B., 2001. Interannual variability of accumulated snow in the Columbia basin, British Columbia. Water Resour. Res. 37, 1753–1759.
Huntington, T.G., 2006. Evidence for intensification of the global water cycle: Review and synthesis. J. Hydrol. 319, 83–95.
Jackson, J.E., 2003. A User's Guide to Principle Components. John Wiley and Sons Inc., Hoboken, New Jersey; 569p.
Jackson, S.I., Prowse, T.D., 2009. Spatial variation of snowmelt and sublimation in a high-elevation, semi-arid basin of Western Canada. Hydrol. Proc. 23, 2611–2627.
Jin, J., Miller, N.L., Sorooshian, S., Gao, X., 2006. Relationship between atmospheric circulation and snowpack in the western USA. Hydrol. Proc. 20, 753–767.
Jordan, R., 1991. A one-dimensional temperature model for a snow cover: Technical documentation for SNTHERM.89. Special Report 91-16, US Army Cold Research and Engineering Laboratory: Hanover, NH: 58p.
Kendall, M.G., 1975. Rank Correlation Methods. Charles Griffin, London.
Kiem, A.S., Franks, S.W., 2001. On the identification of ENSO-induced rainfall and runoff variability: a comparison of methods and indices. Hydrol. Sci. J. 46, 715–727.
Kim, J.-S., Jain, S., Norton, S.A., 2010. Streamflow variability and hydroclimatic change at the Bear Brook Watershed in Maine (BBWM), USA. Environ. Monit. Assess. http://dx.doi.org/10.1007/s10661-010-1525-1.
Kustas, W.P., Brutsaert, W., 1986. Wind profile constants in a neutral atmospheric boundary layer over complex terrain. Boundary Layer Meteorol. 34, 35–54.
Lemke, P., Ren, J., Alley, R.B., Allison, I., Carrasco, J., Flato, G., Fujii, Y., Kaser, G., Mote, P., Thomas, R.H., Zhang, T., 2007. Observations: Changes in Snow, Ice and Frozen Ground. In: Climate Change 2007: The Physical Science Basis. Contribution of Working Group 1 to the Fourth Assessment Report of the Intergovernmental Panel on Climate Change. Cambridge University Press, Cambridge, UK and New York, NY, USA. pp. 337–384.
Lundquist, J.D., Minder, J.R., Neiman, P.J., Sukovich, E., 2010. Relationships between Barrier Jet Heights, orographic precipitation gradients, and streamflow in the Northern Sierra Nevada. J. Hydrometeorol. 11, 1141–1156.
Mann, H.B., 1945. Non-parametric tests against trend. Econometrica 13, 245–259.
Mantua, N.J., Hare, S.R., Zhang, Y., Wallace, J.M., Francis, R.C., 1997. A Pacific interdecadal climate oscillation with impacts on salmon production. Bull. Am. Meteorol. Soc. 78, 1069–1079.
Mawdsley, J.A., Brutsaert, W., 1977. Determination of regional evapotranspiration from upper air meteorological data. Water Resour. Res. 13, 539–548.
McCabe, G.J., Clark, M.P., 2005. Trends and variability in snowmelt runoff in the western United States. J. Hydrometeorol. 6, 476–482.
McCabe, G.J., Dettinger, M.D., 2002. Primary modes and predictability of year-to-year snowpack variations in the western united states from teleconnections with Pacific Ocean Climate. J. Hydrometeorol. 3, 13–25.
McCabe, G.J., Wolock, D.M., 2010. Long-term variability in Northern Hemisphere snow cover and associations with warmer winters. Clim. Chang. 99, 141–153.
Merritt, W.S., Alila, Y., Barton, M., Taylor, B., Cohen, S., Neilsen, D., 2006. Hydrologic response to scenarios of climate change in sub watersheds of the Okanagan Basin, British Columbia. J. Hydrol. 326, 79–108.
Moore, R.D., McKendry, I.G., 1996. Spring snowpack anomaly patterns and winter climatic variability, British Columbia, Canada. Water Resour. Res. 32, 623–632.
Mote, P.W., 2003. Trends in snow water equivalent in the Pacific Northwest and their climatic causes. Geophys. Res. Let. 30, 1–4.
Myers, D.R., 2005. Solar radiation modeling and measurements for renewable energy applications: data and model quality. Energy 30, 1517–1531.
Pellicciotti, F., Raschle, T., Huerlimann, T., Carenzo, M., Burlando, P., 2011. Transmission of solar radiation through clouds on melting glaciers: a comparison of parameterizations and their impact on melt modelling. J. Glaciol. 57, 367–381.
Pettitt, A.N., 1979. A non-parametric approach to the change point problem. Appl. Stat. 28, 126–135.
Räisänen, J., 2008. Warmer climate: less or more snow? Clim. Dyn. 30, 307–319.
Regonda, S.K., Rajagopalan, B., Clark, M., Pitlick, J., 2005. Seasonal cycle shifts in hydroclimatology over the Western United States. J. Clim. 18, 372–384.
Romolo, L., Prowse, T.D., Blair, D., Bonsal, B.R., Marsh, P., Martz, L.W., 2006a. The synoptic climate controls on hydrology in the upper reaches of the Peace River Basin. Part II: Snow ablation. Hydrol. Proc. 20, 4113–4129.
Romolo, L., Prowse, T.D., Blair, D., Bonsal, B.R., Martz, L.W., 2006b. The synoptic climate controls on hydrology in the upper reaches of the Peace River Basin. Part I: Snow accumulation. Hydrol. Proc. 20, 4097–4111.
Stahl, K., Moore, R.D., McKendry, I.G., 2006. The role of synoptic-scale circulation in the linkage between large-scale ocean-atmosphere indices and winter surface climate in British Columbia, Canada. Int. J. Climatol. 26, 541–560.
Stewart, I., 2009. Changes in snowpack and snowmelt runoff for key mountain regions. Hydrol. Proc. 23, 78–94.
Stewart, I.T., Cayan, D.R., Dettinger, M.D., 2005. Changes toward earlier streamflow timing across Western North America. J. Clim. 18, 1136–1155.
Sugita, M., Brutsaert, W., 1991. Daily evaporation over a region from lower boundary layer profiles measured with radiosondes. Water Resour. Res. 27, 747–752.
Sugita, M., Brutsaert, W., 1992. LANDSAT surface temperatures and radio soundings to obtain regional surface fluxes. Water Resour. Res. 28, 1675–1679.
Taylor, B., Barton, M., 2004. Chapter 4. Climate. In: Cohen, S., Neilsen, D., Welbourn, R. (Eds.), Expanding the Dialogue on Climate Change and Water Management in the Okanagan Basin. Final Report, British Columbia, pp. 24–45.
Vavrus, S., 2007. The role of terrestrial snow cover in the climate system. Clim. Dyn. 29, 73–88.
Wijngaard, J.B., Klein Tank, A.M.G., Können, G.P., 2003. Homogeneity of 20th century European daily temperature and precipitation series. Int. J. Clim. 23, 679–692.
Wolter, K., Timlin, M.S., 1993. Monitoring ENSO in COADS with a seasonally adjusted principle component index. In: Proceedings of the 17th Climate Diagnostics Workshop, NOAA/NMC/AC, NSSL, Oklahoma Climate Survey, CIMMS and the School of Meteorology. University of Oklahoma.
Wolter, K., Timlin, M.S., 1998. Measuring the strength of ENSO events – how does 1997/98 rank? Weather 53, 315–324.
Wolter, K., Timlin, M.S., 2011. El Nino/Southern oscillation behaviour since 1871 as diagnosed in an extended multivariate ENSO index (MEI.ext). Int. J. Climatol. 31, 1074–1087.
Yue, S., Pilon, P., Phinney, B., Cavadias, G., 2002. The influence of autocorrelation on the ability to detect trend in hydrological series. Hydrological Processes 16, 1807–1829.
Zhang, X., Harvey, K.D., Hogg, W.D., Yuzyk, T.R., 2001. Trends in Canadian streamflow. Water Resour. Res. 37, 987–998.